Constraining Electron Parallel Energy in Electrostatic Fields through the Anomalous Doppler Effect Induced by External Electromagnetic Waves

1.Author Names:
[1] Department One, Institution One, City One, Country One
[2] Department Two, Institution Two, City Two, Country Two
Email:
xxx@xxx.xxx

Please do not include any author names or affiliations anywhere in the manuscript (or any supplementary files)

Do not include any names in file names and ensure document properties are properly anonymised.

Abstract

The interaction between free electrons and electromagnetic waves (EMW) under the influence of magnetic and electrostatic fields is investigated using a Volume-Preserving algorithm. When the electric field of the EMW, containing a left-hand polarization component, exceeds a critical threshold, it facilitates continuous transfer of parallel electron energy into rotational energy through the Anomalous Doppler Effect (ADE). This process transforms the electric field's work along the magnetic field into perpendicular kinetic energy, leading to saturation of the electron's parallel kinetic energy and continuous growth of its perpendicular kinetic energy. A theoretical model based on energy, momentum, and angular momentum conservation elucidates the role of left-hand polarization in the Anomalous Doppler Effect and provides a generalized framework for interpreting electron-wave interactions. This study proposes a novel approach for mitigating runaway electrons in magnetically confined plasmas, suggesting the use of extraordinary waves launched from the high-field side with an energy flux of hundred watts per square meter to saturate parallel energy in Tokamaks.

I. Introduction

In the beginning of burning plasma device discharge (current ramp up phase), the magnetohydrodynamic (MHD) instabilities and disruption can generate quasi-static toroidal electric fields that accelerate electrons to energies reaching several tens of MeV. This acceleration occurs when the force exerted by the quasi-static electric field surpasses the opposing forces from radiation and collisional drag. These high-energy

electrons, known as runaway electrons, can inflict severe damage on the tokamak's interior walls, thereby shortening the device's operational lifespan. An intriguing possibility is to convert the energy gained by electrons from quasi-static electric fields into rotational energy within the magnetic field. This approach not only suppresses the energy of runaway electrons, moderates their harmful impact on the device, but also improves discharge performance by reducing the consumption of ohmic field energy.

The transport of parallel energy from electrons into rotational energy primarily occurs through three different mechanisms, including the electron avalanche process [1], collisionless pitch-angle scattering[2] and the Anomalous Doppler Effect (ADE) [3]. Current strategies to suppress runaway electrons, such as gas injection [4] and the enhancement of magnetic turbulences[5], often have unintended side effects and interrupt the discharge. In contrast, the ADE mechanism provides an attractive approach.

When electron moves in static magnetic fields and interact with external electromagnetic waves (EMW) of frequency ω and wave vector $\vec{k}$, they undergo a scattering phenomenon under the resonant condition $\omega - \vec{k} \cdot \vec{v} = m\omega_{ce}$, where m is integral number and m<0, ω_{ce} refers to electron cycltron frequency and $\omega_{ce} > 0$, $\vec{v}$ refers to the electron velocity. This scattering results in the transfer of momentum from parallel motion to rotational motion. This phenomenon, known as the Anomalous Doppler Effect, was first thoroughly described in the seminal works of Ginzburg and Frank [3, 6, 7].Recently, the ADE has garnered increasing attention in fields such as space radiation[8], runaway electron instabilities[9], and materials science [10]. It is believed that ADE can explain phenomena like whistler turbulence in solar flare loops [8], the step-like structure in Electron Cyclotron Emission (ECE) observed in tokamaks [11-13], and the microwave bursts during Edge Localized Modes (ELMs) [14]. Furthermore, Anomalous Doppler Effect has shown potential for suppressing runaway electron energy in tokamak discharges.This potential was demonstrated by F. Santini [15], who found that high-energy runaway electrons could be significantly reduced through Anomalous Doppler Effect during lower hybrid wave heating in the Frascati Tokamak. However, it is important to note that the high power of lower hybrid waves also increases the high energy tail of electrons electron energy distribution functions through Landau resonance, leading to a subsequent rise in runaway electrons after the lower hybrid waves are turned off. This side effect poses a challenge to the use of lower hybrid waves for suppressing runaway electrons.

Additionally, the experiment conducted by E.G. Shustin [16] demonstrated that the transverse energy of electrons increases significantly through the Anomalous Doppler Effect when the electron beam of energy 1.5-2 keV and current 60-100 mA in a discharge tubeexcites waves within the frequency range between the electron cyclotron frequency and the upper hybrid frequency. This intrinsic plasma wave is generated via wave-particle interactions, resulting in the scattering of the electron beam's parallel velocity into the perpendicular direction. Furthermore, C. Liu [9] investigated runaway kinetic instability using the kinetic equation and observed that when whistler waves are excited, they cause the scattering of runaway electrons via the Anomalous Doppler Effect. Similar findings include the runaway scattering effect observed on HT-7 [17] and FTU [18], as well as energetic electron scattering in solar flare loops [8]. These waves can not only be generated through wave-particle interactions but also through external injection.The loop of electron acceleration, wave excitation,scattering and energy suppression typically breaks at wave excitation due to damping from thermal electrons and Landau damping, which weakens the exicited wave intensity and limits its ability to scatter runaway electron energy effectively. Consequently, suppressing the parallel energy of runaway electrons through the Anomalous Doppler Effect by injecting specific electromagnetic waves appears to be a natural approach. While a previous study has proposed using whistler waves to suppress runaway electrons based on simulations with the quasilinear kinetic equation [19], further explorations and investigations are still required to fully comprehend and optimize this approach for practical applications.

Understanding the Anomalous Doppler Effect in the presence of electrostatic fields is essential for comprehending the physics of pitch-angle scattering of runaway electrons by electromagnetic waves in Tokamak discharges. Additionally, the basic physics of Anomalous Doppler Effect remains intricacy to understand. It is still lacking a clear physical understanding of why parallel kinetic energy can convert into transverse internal energy during Anomalous Doppler Effect resonance, and what kind of electromagnetic waves can trigger velocity scattering. Despite that the Anomalous Doppler Effect has been explored in either based on the test particle [20] or quasilinear kinetic equation [21-23], these questions still remain to be answered. In this paper, test electrons are used to investigate the Anomalous Doppler Effect in an effort to address the question outlined above. A theoretical model based on energy, momentum, and angular momentum conservation is proposed to explain the role of left-hand polarization in the Anomalous Doppler Effect. This model is provided in the appendix for reference to ensure that the main discussion in the paper remains cohesive and uninterrupted.

This paper presents a direct simulation of full orbit electron motion in uniform magnetic fields, along with accelerating electrostatic field and external electromagnetic field, using the Volume-Preserving Algorithm [24]. Compared to conventional algorithms like Boris [25], the Volume-Preserving Algorithm ensures long-term accuracy and

conservativeness through a systematic splitting method, making it an ideal approach for nonlinear electron dynamic simulations. To directly observe the Anomalous Doppler ffect, an electron is placed in a uniform magnetic field and an electrostatic field, which is oriented opposite to background magnetic field. This setup allows the electron to be accelerated parallel to background magnetic field. During the simulation, a slow electromagnetic wave with a phase velocity smaller than that of light in vacuum is introduced as an external wave. This wave enables us to inverstigate the effects when the electron's velocity reaches the resonant condition for the Anomalous Doppler Effect. We explore resonance with three types of polarization waves: linear polarization, left-hand circular polarization, and right-hand circular polarization. The results show that only the wave with left-hand circular polarization induces the Anomalous Doppler Effect for runaway electrons. The simulation also reveals the critical energy of waves above which the electron's parallel velocity is constrained and parallel energy obtained from the electrostatic field is consistently transfered to transverse rotational energy. Furthermore, the self-consistency between quantum theory and direct simulation of the Anomalous Doppler Effect is examined. Through the analysis of dispersion, polarization, and resonant moments, we determine that the extraordinary wave is most suitable for triggering the Anomalous Doppler Effect in plasma. Based on these findings, we propose an effective method for controlling runaway electrons.

The numerical simulation framework and results are presented in Section II. The trapping threshold is examined in Section III. Section IV explores the dynamics of electromagnetic waves driving the Anomalous Doppler Effect in magnetized plasma. The runaway electron suppression method using extraordinary wave injection is introduced in Section V. Finally, the summary is provided in Section VI.

II. Numerical Simulation Framework and Result Discussion

The uniform magnetic field $\vec{B}_0$ is set on the z-direction. The electron is accelerated by the electrostatic field $\vec{E}_0$, which on the opposite direction to $\vec{B}_0$ as shown in Fig. 4. A plane electromagnetic wave-field is established in the plasma, which characterized by frequency ω and wavevector $\vec{k}$. The electron orbit and motion p in this scenario is presented as eq. (1). The vectors **E** and **B** represent the total fields, which include both static and electromagnetic components. The variable **p** denotes the momentum, c is the speed of light in vacuum, r represents the electron's position, e denotes the electron's charge and m_0 is the electron's rest mass.
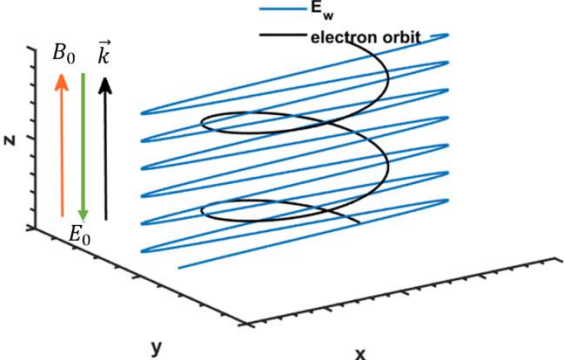
$$
\frac{d\mathbf{r}}{dt} = \frac{\mathbf{p}}{\sqrt{m_0^2 + \frac{\mathbf{p}^2}{c^2}}}
$$

$$
\frac{d\mathbf{p}}{dt} = -e\left(\mathbf{E}(r,t) + \frac{\mathbf{p}}{\sqrt{m_0^2 + \frac{\mathbf{p}^2}{c^2}}} \times \mathbf{B}(r,t) \right) \tag{1}
$$

Figure 1. The uniform background magnetic is set on z direction (orange). The electrostatic field is marked with green. The electromagnetic field propagates along z direction , with the linear polarization along x direction and electric field intensity E_w. The electron orbit has been plotted in black.

The discrete structure of eq. **Error! Reference source not found.** is rewritten as eq. (2) by employing the Volume-Preserving Algorithm [24, 26, 27], here the k is the iteration step and the operator Cay(A) denotes the Cayley transform of matrix A [24].

$$
\begin{cases}
\mathbf{r}^*_{k+\frac{1}{2}} = \mathbf{r}^*_k + \frac{\Delta t^*}{2}\frac{\mathbf{p}^*_k}{\gamma_k}, \\[2mm]
\mathbf{p}^{*-} = \mathbf{p}^*_k + \frac{\Delta t^*}{2}\mathbf{E}^*_{k+\frac{1}{2}}, \\[2mm]
\mathbf{p}^{*+} = \mathrm{Cay}\left(\frac{\Delta t^* \widehat{B^*}}{2\gamma^{*-}}\right)\mathbf{p}^{*-} \\[2mm]
\mathbf{p}^*_{k+1} = \mathbf{p}^{*+} + \frac{\Delta t^*}{2}\mathbf{E}^*_{k+\frac{1}{2}}, \\[2mm]
\mathbf{r}^*_{k+1} = \mathbf{r}^*_{k+\frac{1}{2}} + \frac{\Delta t^*}{2}\frac{\mathbf{p}^*_{k+1}}{\gamma_{k+1}},
\end{cases}
\tag{2}
$$

The dimensionless magnetic matrix $\widehat{B}^*$ is presented as eq. (3).

$$
\widehat{B}^* = \begin{pmatrix} 0 & B_z^* & -B_y^* \\ -B_z^* & 0 & B_x^* \\ B_y^* & -B_x^* & 0 \end{pmatrix}
\tag{3}
$$

The dimensionless parameters are momentum $p^* = p/(m_e c)$, magnetic field $B^* = B/(\frac{m_e}{e\tau_{ce}})$, total electric field $E^* = E/(\frac{m_e c}{\tau_{ce} e})$, time step $\Delta t^* = \Delta t/\tau_{ce}$, and position $x^* = x/(\tau_{ce} c)$ respectively, where the τ_{ce} is the electron cyclotron period and $\gamma^* = \sqrt{1 + p^{*2}}$ is Lorentz factor.

As a preliminary validation calculation, the parameters are set as following: background magnetic field $B_0 = 0.02\ T$, wave angular frequency $\omega_s = 1.5\ \omega_0$ where $\omega_0 = (eB_0)/m_e$, wavevector $\vec{k} = 10^5/m$, the electric field component of the electromagnetic wave $E_w = 9\ V/m$, and the electrostatic field is $E_0 = -2.5\ V$. All these parameters are only set for the purpose of quick simulation. The real tokamak scale calculation will be discussed in the following section. The time step is always chosen to satisfy $\Delta t = min(2\pi/(50(\vec{k} \cdot \vec{v})), 2\pi/50\omega, 2\pi/(50\omega_0))$ to ensure the accuracy of the simulation. The test electron begins at rest and gradually gains speed and the resonant frequency of Normal Doppler effect and Anomalous Doppler effect increases according to eq.(21), and (23).
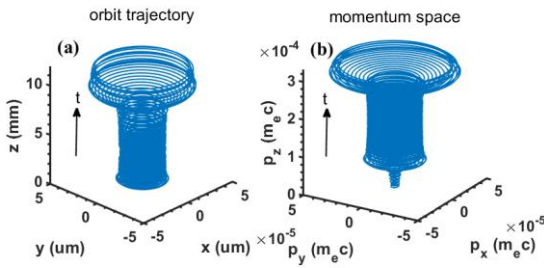

Figure 2. Orbit trajectory of electron motion (left). Momentum phase space of electron motion(right)
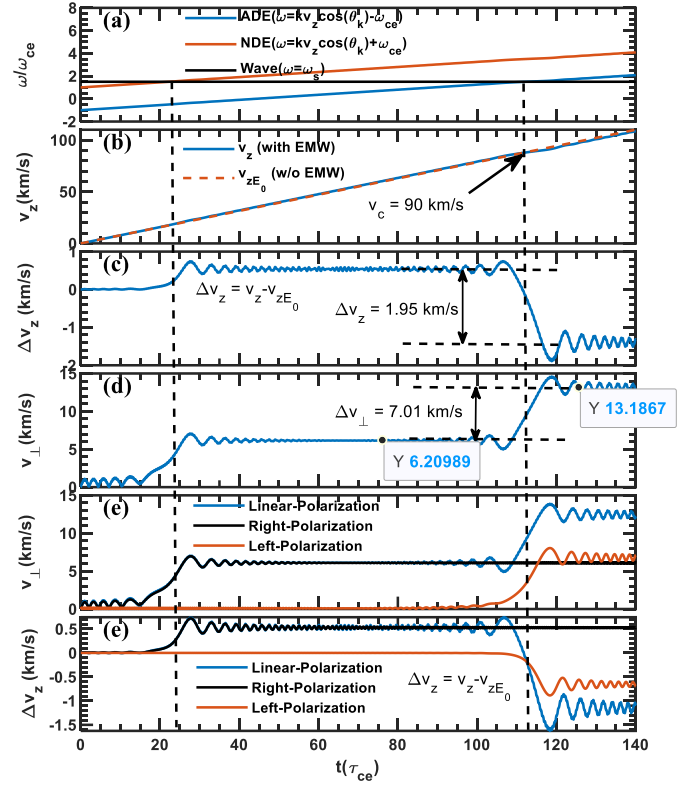

Figure 3. Kinetic evolution of electrons in a magnetic field with electromagnetic wave during acceleration. (a) Wave frequencies of Anomalous Doppler Effect(ADE), Normal Doppler Effect(NDE), and source wave frequency. (b) The parallel velocity v_z in the case with and without the electromagnetic wave. (c) The change of parallel velocity caused by the electromagnetic wave. (d) The cyclotron velocity $v_\perp$. (e) The change of circular velocity during interaction with linear, right-hand circular, and left-hand circular polarization. (f) The change of parallel velocity during interaction with linear, right-hand circular, and left-hand circular polarization.

Figure 2 illustrates the evolution of the electron's orbit and velocity phase during acceleration. The details of the electron's motion are shown in figure 3. As the electron accelerates in the electrostatic field (figure 3(b)), the resonant frequencies increase concurrently (figure 3(a)). At around $23\tau_{ce}$, when the Normal Doppler Frequency matches that of the induced wave, the perpendicular velocity (or rotational velocity) $v_\perp$ increases rapidly (figure 3(d)). The parallel velocity v_z induced by the electromagnetic wave also increases, as shown in figure 3(c). This change can be calculated as $\Delta v_z = v_z - v_{zE0}$, where v_z is the parallel velocity due to both the electromagnetic wave and the electrostatic field, while v_{zE0} is the parallel velocity resulting only from the electrostatic field.

This phenomenon corresponds to the Normal Doppler Effect, where the resonant velocity $v_{NDE} = (\omega - \omega_{ce})/k_z < c'$ is "subluminal." The absorption of induced waves by the cyclotron electron results in an increase in both parallel and perpendicular velocities, which can be considered a reverse process to the photon emission described in the appendix. The Normal Doppler Effect process is widely used for current drive [28] and plasma heating [29] in tokamaks. However, it is generally believed that current drive via electromagnetic waves follows the Fisch mechanism [30], due to the limited toroidal momentum injected by the waves.

The resonant condition is quickly disrupted as the parallel velocity continues to increase until it reaches $v_{ADE} = (\omega + \omega_{ce})/k_z$, at which point the Anomalous Doppler Effect begins to emerge. When the time reaches $113\,\tau_{ce}$, the system starts resonating with the induced wave through the Anomalous Doppler Effect, where $\omega_{ADE} = \omega$ as shown in figure 3(a). At this point, the parallel velocity begins to scatter into the perpendicular direction, evident from the decrease in Δv_z and the increase in $v_\perp$ as seen in figure 3(c) and figure 3(d). The resonant condition rapidly disappears as the parallel velocity exceeds the resonant region. During the resonant period, the changes in perpendicular and parallel energies are calculated as $\Delta E_\perp = \frac{1}{2} m_e \Delta v_\perp^2 \approx 6.1556 \cdot 10^{-23}\,J$ and $\Delta E_{||} = \frac{1}{2} m_e \Delta v_z^2 = m_e \Delta v_z v_c \approx -1.5987 \cdot 10^{-22}$ J respectively, as shown in figure 3(c) and figure 3(d). The ratio of the energy changes is $\Delta E_\perp / \Delta E_{||} \approx -0.385$. According to quantum theory, as derived in Appendix eq. (19), the change ratio of $\Delta U_{21}/\Delta T_{21} = -\hbar \omega_{ce}/\hbar \vec{k} \cdot \vec{v} = -0.3908$, where $\omega_{ce} \approx 3.5176 \cdot 10^9/s$, and k = 10^5 /m, v = 90 km/s. The quantum theory results are in good agreement with the numerical calculations.
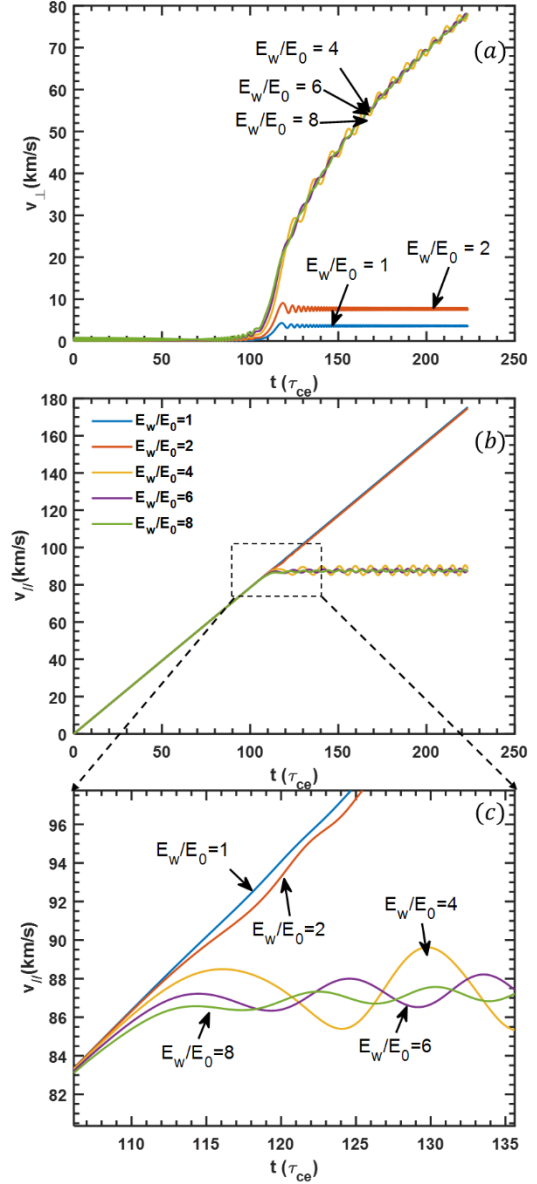

Figure 4. Time trace of velocity under different ratios of E_p/E_0. (a) Vertical velocity, (b) Parallel velocity, (c) Zoom in parallel velocity.

To determine which type of electromagnetic wave is responsible for the Normal Doppler Effect, and the Anomalous Doppler Effect separately, we decompose the linearly polarized wave into left-handed and right-handed circular polarizations. We observe that the right-hand circular polarized wave is responsible for the Normal Doppler Effect, while the left-hand circularly polarized wave induces the Anomalous Doppler Effect, as shown in figure 3(e) and figure 3(f), which aligns well with our analysis in appendix.

This phenomenon is understood through the conservation of angular momentum and momentum. The electron exhibits right-hand circular polarization of its orbital motion in a

magnetic field. When an electron absorbs right-hand circularly polarized electromagnetic waves propagating parallel to the magnetic field, the conservation of momentum and angular momentum causes an increase in the electron's parallel momentum and rotational energy, corresponding to the Normal Doppler Effect. Conversely, when the electron emits left-hand circularly polarized electromagnetic waves propagating parallel to the magnetic field, the conservation of momentum results in a decrease in the electron's parallel momentum, while the conservation of angular momentum leads to an increase in its rotational energy, corresponding to the Anomalous Doppler Effect. It is important to note that the Cherenkov effect does not involve electromagnetic waves, as it is primarily associated with electrostatic waves.

We observe that when the Anomalous Doppler Effect (ADE) occurs at $113\tau_{ce}$, a portion of the parallel velocity is scattered into the cyclotron velocity, as shown in figure 3(e) and figure 3(f). Despite this scattering, the parallel velocity continues to increase due to the influence of the background accelerating electrostatic field, eventually exceeding the resonant velocity, as illustrated in figure 3(b). If the parallel velocity increase driven by the electrostatic field could be efficiently and timely redirected into the cyclotron velocity, it may be possible to trap the parallel velocity and prevent its further escalation.

III. Critical Trapping Threshold of Anomalous Doppler Effect

The Anomalous Doppler Effect functions as an effective damping force that impedes the electron acceleration process. By increasing the intensity of the electromagnetic wave, it is theoretically possible to balance the electrostatic field force, preventing further electron acceleration by the electrostatic field. The existence of this equilibrium will be demonstrated by varying the electromagnetic wave field intensity.

An electromagnetic wave with only a left-hand polarized circular component is considered, characterized by a wave vector $k = 10^5/m$ and frequency $\omega = 1.5\,\omega_0$, where $\omega_0 = (eB_0)/m_0$, refers to the electron cyclotron frequency in rest frame and k is aligned parallel to the static magnetic field. The electrostatic field and static magnetic field are set to $E_0 = -2.5\,V$ and $B_0 = 0.02\,T$, respectively. As shown in figure 4, increasing the energy of the electromagnetic wave results in the parallel velocity becoming trapped in the resonant condition, ceasing to increase, as shown in figure 4(b) and figure 4(c) while the perpendicular velocity continues to rise once the ratio E_w/E_0 exceeds a specific threshold (figure 4(a)). The electron's orbit and momentum of the trapped electron are illustrated in figure 5.

The threshold field E_c can be determined by adjusting the electromagnetic wave intensity using a dichotomy control method, based on the final parallel velocity over a sufficiently

long time. The critical ratios E_c/E_0 as functions of the dimensionless parameter $\frac{\omega^2}{kc\omega_0}$ are shown in figure 6, with the angles between B_0 and the wave vector k set at $\theta = 0, 15^o, \text{and } 30^o$. When the magnetic field strength B and wave frequency ω are held constant, a decrease in the wave vector k results in a higher critical field strength. This is because a lower k corresponds to a higher resonant velocity, leading to an increase in the power imparted by the static electric field, $P = E_0 e v_z$. Consequently, a stronger electromagnetic wave intensity is required to achieve timely conversion of parallel energy.

With only a weak left-hand circularly polarized wave, it is possible to halt the increase in the electron's parallel momentum and transfer energy from the electrostatic field to rotational energy via the Anomalous Doppler Effect. For instance, in tokamaks, where the toroidal electric field is approximately 0.2 V/m, the threshold electric field for a left-hand circularly polarized wave to trap parallel energy is around $E_w = 2\,V/m$ in the plasma. This corresponds to an energy flux of approximately $0.04\,W/m^2$ for $k = 2 \times 10^3/$m, and $\omega = \omega_{ce}$ with 0.02 T background magnetic field.
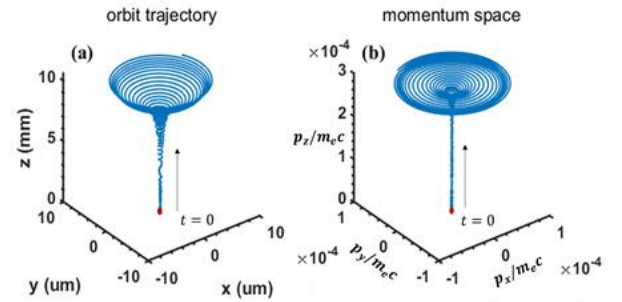

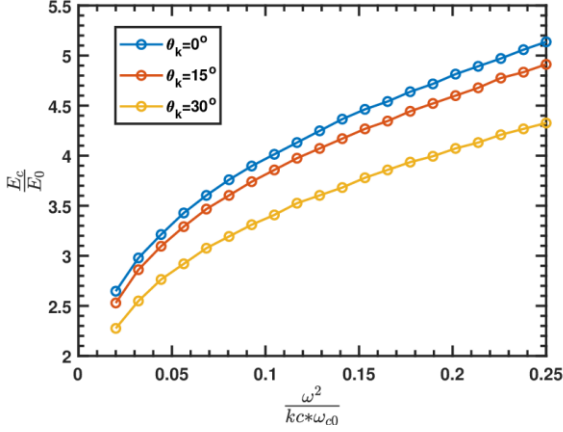Figure 5. The electron's orbit and momentum with trapped parallel energy

Figure 6. The critical ratio of E_c/E_0 with the nomalized parameter $\frac{\omega^2}{kc\omega_0}$. The $E_0 = -2.5$ V , $B_0 = 2 \times 10^{-2}$ T, $\omega = 1.5\ \omega_0$. The refractive index range is set from 4 to 50.

To validate the Anomalous Doppler Effect in high magnetic fields and assess its angle dependence, we consider a uniform magnetic field of B = 2 T and an electrostatic field $E_0 = -0.2$ V/m, representative of typical tokamak startup conditions [9]. For a plane left-hand circularly polarized wave with parameters $f = 56$ GHz, $E_w = 40$ V/m, and k = 2.6×10^3/m, the wave's energy flux is approximately 9 W/m². Utilizing the computational parallelism of a supercomputer, we simulate the interaction of 500 electrons with the wave at 500 distinct incident angles θ ranging from 0 to 90 degrees, thereby elucidating the angle dependence of the Anomalous Doppler Effect . The ratio of $E_w/E_0 = 200$ significantly exceeds the critical threshold of approximately 5, ensuring that electrons' parallel velocity at all incident wave angles is trapped once it reaches the velocity at Anomalous Doppler resonance.

The simulation employs a time step of $\Delta t = 1 \times 10^{-14}$ s to ensure result convergence. The outcomes are depicted in figure 7, where the dashed yellow line indicates the earliest resonant time satisfying the condition $\omega - \vec{k} \cdot \vec{v} + \omega_{ce} = 0$. The results reveal that as θ_k increases, the onset of resonance is delayed, and the velocity required for resonance becomes higher. Once resonance begins, the rotational velocity $v_\perp$ increases rapidly, while the parallel velocity becomes trapped in the resonant region, halting further growth.
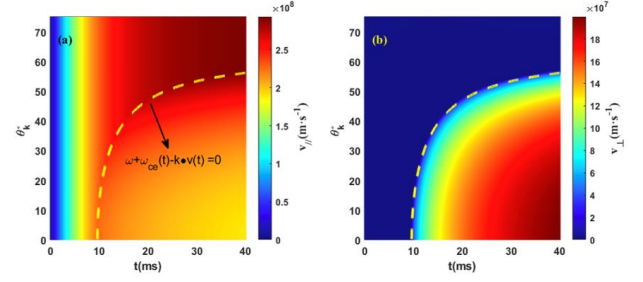

Figure 7. Time evolution of $v_\perp$ (left) and $v_\parallel$ (right) by electromagnetic wave with different wave incident angle θ_k^o.

IV. Electromagnetic wave drives the Anomalous Doppler Effect in magnetized plasma

Runaway electrons pose a severe risk to tokamak devices, as their high-energy impacts can cause substantial damage to plasma-facing components (PFCs) [31]. Leveraging the Anomalous Doppler Effect within tokamaks provides a viable strategy for mitigating runaway electron energy, contingent upon satisfying three essential conditions. By fulfilling these criteria, it is possible to establish controlled resonant interactions, offering an effective means of suppressing runaway electrons.
1. The presence of a left-hand polarized wave component aligned with the electron motion in the magnetic field direction.
2. The phase velocity of the electromagnetic wave must remain subluminal, i.e., below the speed of light in a vacuum.
3. The wave must carry sufficient energy to counterbalance the accelerating velocity of the electrons.

The injection of an electromagnetic wave would naturally couple with the plasma, transforming into a combination of its intrinsic wave modes within plasma. The cold magnetized plasmas dispersion is valid when the phase velocity significantly exceeds the thermal velocity of electrons. The dispersion relation for a cold plasma in a magnetized medium is expressed as eq.(4).

$$
\begin{aligned}
&\omega^{10} - \omega^8\left(2k^2c^2 + \omega_{ce}^2 + \omega_{ci}^2 + 3\omega_{pe}^2\right) \\
&+\omega^6\left[k^4c^4 + \left(2k^2c^2 + \omega_{pe}^2\right)\left(\omega_{ci}^2 + \omega_{pe}^2\right) + \left(\omega_{pe}^2 + \omega_{ce}\omega_{ci}\right)^2\right] \\
&-\omega^4[k^4c^4\left(\omega_{ce}^2 + \omega_{ci}^2 + \omega_{pe}^2\right) + 2k^2c^2\left(\omega_{pe}^4 + \omega_{ce}\omega_{ci}\right)^2 \\
&+k^2c^2\omega_{pe}^2\left(\omega_{ce}^2 + \omega_{ci}^2 - \omega_{ce}\omega_{ci}\right)(1 + \cos^2\theta) \\
&+\omega_{pe}^2\left(\omega_{pe}^2 + \omega_{ce}\omega_{ci}\right)^2] + \omega^2[k^4c^4\omega_{pe}^2\cos^2\theta \\
&+k^2c^2\omega_{pe}\omega_{ce}\omega_{ci}\left(\omega_{pe} + \omega_{ce}\omega_{ci}\right)(1 + \cos^2\theta)] \\
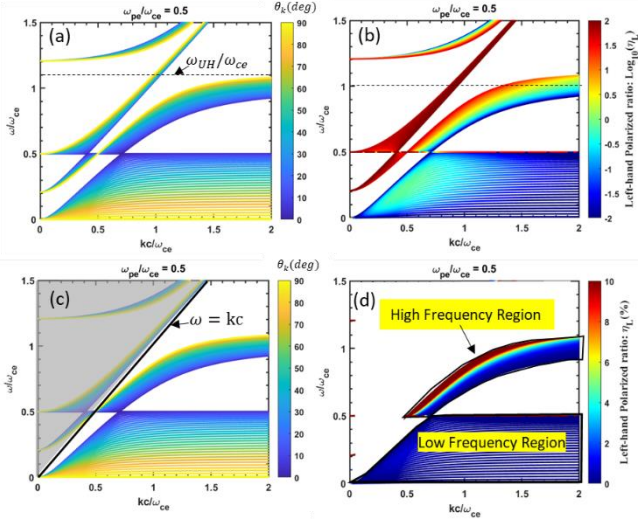&-k^4c^4\omega_{ce}^2\omega_{ci}^2\omega_{pe}^2\cos^2\theta = 0
\end{aligned} \tag{4}
$$

Figure 8.Dispersion relationship in cold magnetized plasma. ω_{UH} refers to the upper hybrid frequency. (a) Complete dispersion relationship in cold magnetized plasma. (b) The ratio of Left-hand polarized wave in cold plasma dispersion. (c) Region where the phase velocity is smaller than the speed of light in vacuum. (d) High-frequency and low-frequency regions.

The relationship of ω and k depend on the electron cyclotron frequency(ω_{ce}), the plasma frequency (ω_{pe}) and the ion cyclotron frequency(ω_{ci}). Here, θ is the angle between $\vec{k}$ and the static magnetic field $\vec{B}$. Considering the case where $\omega_{pe}/\omega_{ce} = 0.5$, the dispersion relationship can be illustrated in figure 8(a), where the blue color represents the wavevector $\theta = 0$, while the yellow color represents $\theta = 90$ degrees. The polarization component in direction (e_x, e_y, e_z) of the wave can be expressed as [32]:

$$(A, iB, C) = \left(1, i\frac{\frac{\omega_{pe}^2 \omega_{ce}}{\omega}}{\omega^2 - k^2 c^2 - \omega_{ce}^2 - \omega_{pe}^2 + \frac{k^2 c^2 \omega_{ce}^2}{\omega^2}}, \frac{k_\parallel k_\perp c^2}{\omega_{pe}^2 + k_\perp^2 c^2 - \omega^2}\right) \quad (5)$$

Here, the vector e_z is aligned with the magnetic field, while e_x and e_y are orthogonal vectors lying in the plane perpendicular to the magnetic field.The electric field of the wave is expressed as $\vec{E} = E_0\left(Ae_x + iBe_y + Ce_z\right)\exp(i(\vec{k} \cdot \vec{r} - wt))$. For a wave propagating along the z-axis, the left-hand polarized wave is represented as $E_L = \left(e_x - ie_y\right)exp\left(i(k \cdot z - \omega t)\right)$. When the left-hand polarized wave propagates along the k direction, with k lying in the x-z plane, the polarization component of the left-hand polarized wave, as determined by the rotation matrix about the x-axis, is given by:

$$E_L = \begin{bmatrix} E_x \\ E_y \\ E_z \end{bmatrix} = \begin{bmatrix} \cos(\theta) & 0 & \sin(\theta) \\ 0 & 1 & 0 \\ -\sin(\theta_k) & 0 & \cos(\theta_k) \end{bmatrix} \cdot \begin{bmatrix} 1 \\ -i \\ 0 \end{bmatrix} \quad (6)$$

Here, θ_k represents the angle between the wavevector k and the z-axis. The left-hand polarized wave component is caluculated as:

$$\eta_L = \left|\frac{E_L \cdot E^*}{||E_L| \cdot |E|}\right|^2 = \left(\frac{Acos(\theta_k) - B - Csin(\theta_k)}{|E_L| \cdot |E|}\right)^2 \quad (7)$$

The ratio of the left-hand polarized wave in the cold plasma dispersion is shown in figure 8(b), where the region dominated by the left-hand polarized wave can be observed. In figure 8(c), the black line represents waves in a vacuum. Only waves below this line, where the phase velocity $v_p =$

When the runaway electron's momentum satisfies the resonant condition (eq. (8)), it can excite intrinsic waves in the plasma. For simplification, we assume the velocity is aligned with the static magnetic field. In this analysis, we consider n=1 for the Anomalous Doppler Effect, and n=0 for Landau resonance. The case of n = −1 is excluded because the
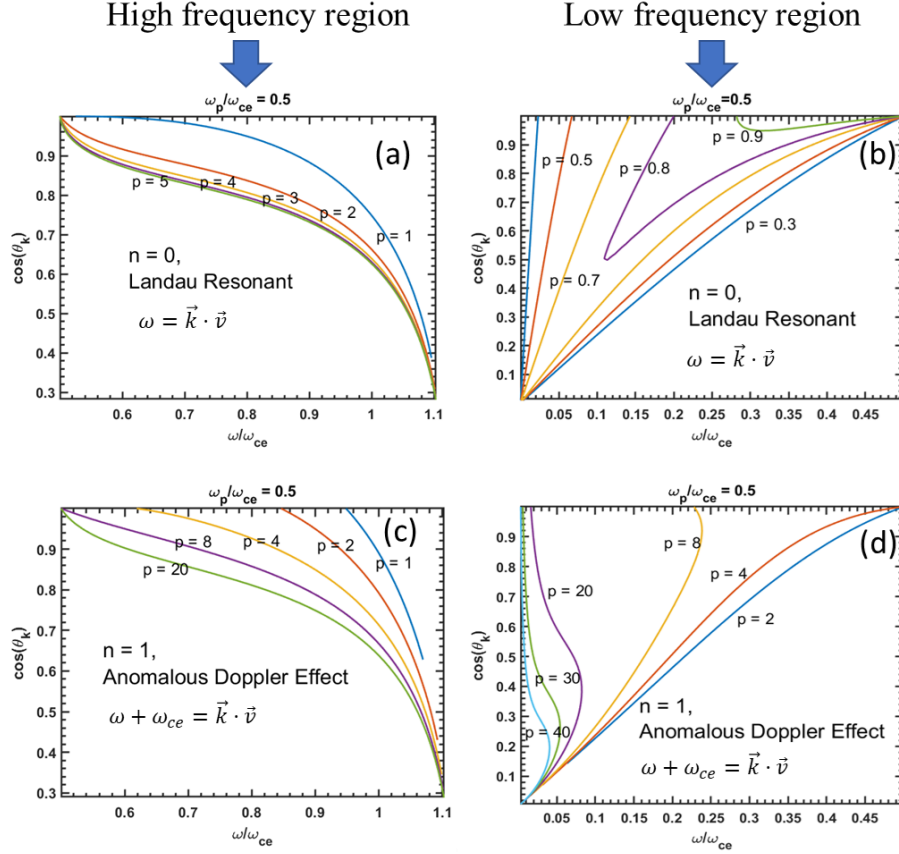

Figure 9. In the high-frequency region, the lower-left boundary represents the upper hybrid wave at various angles. In the low-frequency region, the lower-right boundary corresponds to the lower hybrid wave at different angles. Panels (a) and (b) depict the dimensionless momentum for Landau resonance in the high-frequency region. Panels (c) and (d) illustrate the dimensionless momentum for the Anomalous Doppler Effect (ADE) in both high- and low-frequency regions. The unit for dimensionless momentum is expressed as $m_e c$.

$\frac{w}{k} < c$, can drive the Anomalous Doppler Effect (ADE). Finally, as depicted in figure 8(d), Anomalous Doppler Effect supporting waves are observed in both low- and high-frequency regions

- In the low-frequency region, which includes whistler waves and lower hybrid waves, the ratio of the left-hand polarized wave is below 1%.
- In the high-frequency region, when the angle θ is close proximity to 90 degrees, as shown in figure 8 (d), the ratio of left hand polzrized wave is above 6 %, where it contains extraordinary waves.

$$\omega + n\omega_{ce} - \vec{k} \cdot \vec{v} = 0 \qquad (8)$$

Normal Doppler Effect is not significant in the high-frequency region, as it requires a right-hand polarized wave. By combining eq. (4) and eq. (8), we derive the relationship between the wave properties and the resonant momentum, which is depicted in figure 9.

In the high-frequency region for Anomalous Doppler Effect, resonance curves with dimensionless resonance momentum greater than unity converge to the bottom-right region shown in figure 9, which corresponds to the Extraordinary wave with a frequency range of $\left(\omega_{ce}, \sqrt{\omega_{ce}^2 + \omega_{pe}^2}\right)$. This explains the excitation of Extraordinary waves near these frequencies during runaway electron scattering in magnetized devices [14, 16].

Additionally, the dimensionless Landau resonant momentum in most of the low-frequency region is greater than 1, as shown in figure 9(a), suggesting less wave attenuation by background thermal electrons, which facilitates wave formation in the high-frequency region. In the low-frequency region, when the energy of high-energy runaway electrons exceeds 10 MeV (with reduced momentum p > 20), the resonance curves of electromagnetic waves excited by the ADE effect typically pass through the top-left region depicted in figure 9 (d). This region is closely associated with the whistler wave zone, where whistler waves propagate parallel to the magnetic field. Thus, in Tokamak experiments, the observation of whistler waves is typically linked to the detection of high-energy electrons with energies exceeding 10 MeV [33]. In the low-frequency region, the dimensionless Landau resonance momentum is less than unity, as shown in figure 9(b), indicating a higher degree of wave attenuation by background thermal electrons compared to the high-frequency region, making wave formation in this region more challenging.

Based on the above discussion, electromagnetic waves in the high-frequency region are more prone to exciting Anomalous Doppler Resonance due to polarization and damping effects, while waves in the low-frequency region are better suited for heating background electrons through Landau resonance, such as in lower-hybrid wave heating. Experiments have shown that runaway electrons can stimulate extraordinary waves with frequencies in the range ω_{ce} to ω_{UH} through ADE, thereby transferring their parallel energy to rotational energy [14, 16]. Given that the wave can be generated either externally or through wave-particle interactions, this suggests the potential to employ the same process—injecting extraordinary waves—to suppress runaway electrons.

V. Launching Extraordinary Waves in Tokamaks for Runaway Electron Suppression

The characteristic layer in a tokamak plasma is shown in figure 10. Extraordinary waves slow down near the upper-hybrid frequency layer and reflect at the right-hand cut-off frequency layer. It is essential to inject the extraordinary wave from the high-field side of the tokamak, ensuring that the electric field of the electromagnetic wave is perpendicular to the toroidal magnetic field for effective wave launching. This configuration is critical, as the wave would otherwise be reflected at the right cut-off frequency if injected from the lower-field side. Different frequencies correspond to different upper-hybrid frequency layer positions, allowing the frequency of the extraordinary wave to be adjusted to align with regions where runaway events are more likely to occur, such as the core of the tokamak. Since the power requirement for trapping runaway electrons is on the order of watts, it is worth noting that precise frequency adjustments based on real-time plasma density diagnosis are possible to achieve, allowing for alignment with the tokamak core. Assuing that 90% of the wave energy near the upper-hybrid frequency layer is transformed into plasma heating, with only 10% remaining as an electromagnetic wave, and considering the $\eta_L \approx 10\%$ near the upper-hybrid frequency layer as shown in figure 8(d), the required injected power to achieve 9 W/m² of the left-hand polarized wave, as indicated by the simulation results, is approximately 900 W/m². Additionally, electrostatic waves can also contribute to the Anomalous Doppler Effect [34], which may help reduce the power requirements for suppressing runaway electron energy. However, this effect falls outside the scope of this paper.
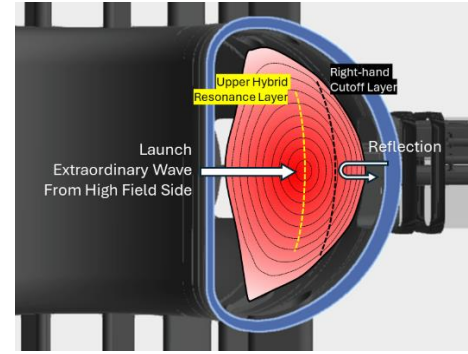

Figure 10. Characteristic frequencies in the tokamak. The Right-hand cutoff layer is on the outside of the Upper Hybrid Resonance Layer.

VII. Summary

The Anomalous Doppler Effect has been identified as an effective mechanism for suppressing runaway electron energy by scattering the electron's parallel energy into perpendicular energy. Through studying the interaction between electrons and electromagnetic waves, this approach offers an innovative solution for runaway electron suppression in tokamaks, requiring a left-hand circularly polarized beam with an intensity of 9 W/m² based on the EAST start-up scenario. In practical tokamak applications, the extraordinary wave predominantly contains left-hand circular polarization components and can be launched from the high-field side of the tokamak. Resonance at the upper hybrid layer drives the Anomalous Doppler Effect within the plasma core, effectively limiting the increase in runaway electron toroidal momentum. Numerical simulations demonstrate that when the electric field exceeds the critical threshold, the electromagnetic wave captures the parallel momentum of the electrons, continuously transferring energy from the parallel electrostatic field to rotational energy and resonant waves.

Appendix. Quantum Theory of the Anomalous Doppler Effect

This extraordinary phenomenon has been previously discussed in terms of energy conservation by V.L. Ginzburg [35], I. Tamm [36], Nezlin [6], and I.M. Frank [7]. In this work, we provide an analysis based on the conservation of angular momentum. As illustrated in figure .11, when charged particles move through a medium at speeds greater than the speed of light in that medium, induced currents are generated. These currents, in turn, stimulate secondary waves that interfere with the electromagnetic field of the moving particles, resulting in Cherenkov radiation. The direction of Cherenkov radiation is constrained to the Cherenkov radiation angle $\theta_0 = \arccos(\frac{c'}{v})$, where c' is the speed of light in the medium and v is the velocity of the charged particles.

In this case, the charged particle is replaced with a system that has internal energy, such as an oscillator or a cyclotron electron in a magnetic field. When the system moves faster than the speed of light ($v > c'$), it emits photons with angular frequency ω and wavevector k in the direction θ. The direction of the emitted photon is not influenced by the interference of secondary waves and can occur in any direction, as shown in figure 12.
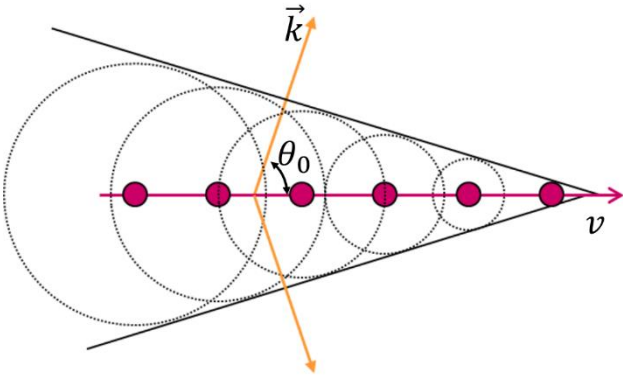

Figure 11. Schematic diagram of Cherenkov Radiation. The red points stand for the snapshot of the electron at different time.
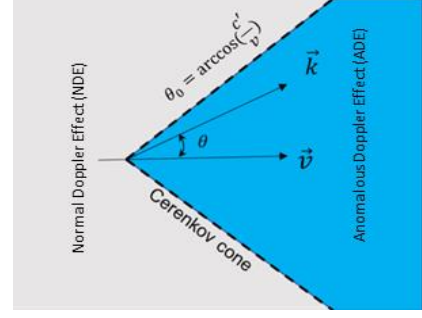

Figure 12.The blue region shows the Anomalous Doppler Effect.

According to energy conservation and momentum conservation:

$$T_1 + U_1 = \hbar\omega + T_2 + U_2 \tag{9}$$

$$\boldsymbol{p}_1 = \boldsymbol{p}_2 + \hbar\boldsymbol{k} \tag{10}$$

In the above, T_1 and U_1 represent the kinetic energy and internal energy of the system before emitting a photon, and T_2 and U_2 represent the energy of the system after emitting a photon, p represents the momentum of the system, k denotes the wavevector of the photon and $\hbar$ represnts reduced Planck's constant. With the assumption that photons energy is far less than the initial kinetic energy T_1, the losses of kinetic energy after emitting a photon can be expressed as $\Delta T_{12} = T_1 - T_2 = \Delta\boldsymbol{p} \cdot \boldsymbol{v}$, where $\boldsymbol{v}$ is the velocity of the system before emitting a photon, and also $\Delta p = \boldsymbol{p}_1 - \boldsymbol{p}_2 = \hbar\boldsymbol{k}$.

$$\begin{aligned}\Delta U_{21} &= \Delta T_{12} - \hbar\omega \\ &= \hbar\vec{k} \cdot \vec{v} - \hbar\omega \\ &= \hbar\omega\left(\frac{kv\cos\theta}{\omega} - 1\right)\end{aligned} \tag{11}$$

Here, $\frac{\omega}{k} = c', \Delta U_{21} = U_2 - U_1$. While the system velocity is greater than the speed of light in the medium ($v > c'$). According to the sign of ΔU_{21}, we can divide radiation into three regions, as shown in figure 12.

- For $\theta > \theta_0 = \arccos\left(\frac{c'}{v}\right)$, $\Delta U_{21} < 0$. The system produces photons by consuming its own internal and kinetic energy, this region refers to the Normal Doppler Effect (NDE).
- For $\theta = \theta_0$, $\Delta U_{21} = 0$, the loss of kinetic energy by the system is completely converted into photon energy; this line refers to the Cerenkov Effect.
- For $\theta < \theta_0$, $\Delta U_{21} > 0$, this region is referred to the Anomalous Doppler Effect (ADE), where the system gains internal energy after emitting photons. It means

the loss of kinetic energy is converted to photons and the system's internal energy.

All three effects are possible when the system velocity exceeds the speed of light ($v > c'$). While the system velocity is less than the speed of light ($v < c'$), only Normal Doppler Effect exists. As observed, the type of phenomenon can be determined by examining the change in internal energy after the emission of photons.

The freely moving electron has a velocity v_z along the background magnetic field and a velocity v_z perpendicular to the magnetic field, as shown in figure 13. The kinetic energy is $T = \gamma m_e c^2 - m_e c^2$. The γ referred to is the Lorentz factor The internal energy represented as $U = \frac{1}{2}\gamma m_e v_\perp^2$. According to the angular momentum conservation, we have
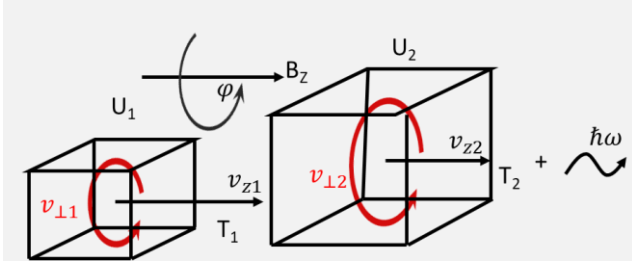
$$L_1 = L_2 + n\hbar \tag{12}$$

Figure 13.Schematic diagram of electron cyclotron system. U₂>U₁, T₂<T₁.

The emitted photon is considered to contain angular momentum of $n\hbar$, and the angular momentum of the cyclotron electron before and after emitting the photon is L_1 and L_2, respectively. Since the magnetic field is aligned along the z-direction, the angular momentum of electron cyclotron along z is represents as L_z.

According to the quantum theory, the electron wave in the static magnetic field can be presented as:

$$\Psi = \Psi_0 e^{\frac{i}{\hbar}(p - eA)\cdot s} \tag{13}$$

With the term Ψ_0 is a normalized coefficient, A is the vector potential and s is the position.

The intrinsic equation of angular momentum in the z-direction has been transformed as

$$-i\hbar \frac{\partial}{\partial \varphi}\Psi = (\boldsymbol{p_\varphi} - e\boldsymbol{A_\varphi})r\Psi \tag{14}$$

$$L_z = (\boldsymbol{p_\varphi} - e\boldsymbol{A_\varphi})r \tag{15}$$

With $p_\varphi = \gamma m_e v_\perp, A_\varphi = \frac{rB_0}{2}$,and $r = \frac{\gamma m_e v_\perp}{B_0 e}$, the eq.(15) is presented as

$$L_z = \frac{1}{2}\frac{\gamma m_0 v_\perp^2}{\omega_{ce}} = \frac{U}{\omega_{ce}} \;, \omega_{ce} = \frac{eB}{m_0 \gamma} = \frac{\omega_0}{\gamma} \tag{16}$$

With m_0 is the electron rest mass, γ is the Lorentz factor and ω_0 is the electron cyclotron frequency in rest frame.

The angular momentum conservation in z direction is $L_{z2} + m\hbar = L_{z1}$. The variation in the angular momentum of the electron along z is presented as

$$\Delta L_{21} = L_{z2} - L_{z1} = \frac{U_2 - U_1}{\omega_{ce}} = -m\hbar \tag{17}$$

With m is the number of photon's angular momentum in z direction.

The internal energy changes $\Delta U_{21} = U_2 - U_1$, with the eq.(17), will be transformed as

$$\Delta U_{21} = -m\hbar\omega_{ce} \tag{18}$$

According to the eq.(11) and eq.(18)(11), the change in electron energy could be presented as

$$\hbar\vec{k} \cdot \vec{v} = \hbar\omega - m\hbar\omega_{ce} \tag{19}$$

$$\omega = k_z v_z + m\omega_{ce} \tag{20}$$

Here, $\hbar\vec{k} \cdot \vec{v}$ represents the loss of kinetic energy ΔT_{12}, $\hbar\omega$ represents the energy of the photon, and $-m\hbar\omega_{ce}$ represents the change in the electron cyclotron energy ΔU_{21} (internal energy change). There are three scenarios about the the internal energy changes.

1. With $m > 0$, $\Delta U_{21} < 0$, the cyclotron electron internal energy decreases after emitting a photon, and the emitted photon will have right-hand circular polarization with angular momentum $m\hbar$ to maintain angular momentum conservation. This process is called the Normal Doppler Effect .
2. For $m = 0, \Delta U_{21} = 0$, the Cherenkov Effect occurs, where the emitted photon does not cause any change in the internal energy of the cyclotron electron.
3. With $m < 0$, $\Delta U_{21} > 0$, the Anomalous Doppler Effect (ADE) occurs,resulting in an increase in the internal energy of the cyclotron electron and the emission of left-hand circular polarization with angular momentum $m\hbar$.

The aforementioned analysis is based on spontaneous emission. However, similar to laser emission, this

conservation model is also applicable to stimulated emission, wherein the emitted photon is generated with the same frequency, direction, and phase as the incident photon. External electromagnetic waves can serve as resonant fields to trigger cyclotron electrons in a magnetic field to emit or absorb waves, providing a framework for analyzing the Anomalous Doppler Effect. For a external electromagnetic wave as plane wave, the wave angular moment number can be devided into $m = \pm 1$. While for $|m| > 1$, it indicates that the resonant wave possesses a helicon structure.

Based on the above discussion,there are three kinds of resonance for a system when electron moves along the uniform magnetic field with velocity v under external EMW :the resonant frequencies are Normal Doppler frequency, Cerenkov frequency , and Anomalous Doppler frequency. We only include the dominate resonance $m = -1, 0, \text{and} + 1$.
Normal Doppler Effect frequency:
$$\omega_{NDE} = kv_z\cos\theta + \omega_{ce} \tag{21}$$
Cerenkov Effect frequency:
$$\omega_{Cerenkov} = kv_z\cos\theta \tag{22}$$
Anoumalous Doppler Effect frequency:
$$\omega_{ADE} = kv_z\cos\theta - \omega_{ce} \tag{23}$$
With θ is the angle between background mangetic field $\vec{B}$ and wavevector $\vec{k}$. These equations are quite common resonant conditions for the kinetic equation of plasma ,what is intriguing is how the motion of electrons differs under various resonant conditions with an electrostatic field.

References

[1] Rosenbluth M and Putvinski S 1997 Theory for avalanche of runaway electrons in tokamaks *Nuclear fusion* **37** 1355

[2] Liu J, Wang Y and Qin H 2016 Collisionless pitch-angle scattering of runaway electrons *Nuclear Fusion* **56** 064002

[3] Ginzburg V L 1960 Certain theoretical aspects of radiation due to superluminal motion in a medium *Soviet Physics Uspekhi* **2** 874

[4] Wei Y, Yan W, Chen Z, Tong R, Jiang Z, Yang Z and team J-T 2019 Runaway current suppression by secondary massive gas injection during the disruption mitigation phase on J-TEXT *Plasma Physics and Controlled Fusion* **61** 084003

[5] Zeng L 2013 Experimental observation of a magnetic-turbulence threshold for runaway-electron generation in the TEXTOR tokamak *PHYSICAL REVIEW LETTERS* **110**

[6] Nezlin M V 1976 Negative-energy waves and the anomalous Doppler effect *Soviet Physics Uspekhi* **19** 946

[7] Frank I 1960 Optics of Light Sources Moving in Refractive Media: Vavilov-Cherenkov radiation, though interesting, is but an experimental instance of a more general problem *Science* **131** 702-12

[8] Filatov L and Melnikov V 2021 The Role of the Anomalous Doppler Effect in the Interaction of Energetic Electrons with Whistler Turbulence in Flare Loops *Geomagnetism and Aeronomy* **61** 1183-8

[9] Liu C, Hirvijoki E, Fu G-Y, Brennan D P, Bhattacharjee A and Paz-Soldan C 2018 Role of kinetic instability in runaway-electron avalanches and elevated critical electric fields *Physical review letters* **120** 265001

[10] Shi X, Lin X, Kaminer I, Gao F, Yang Z, Joannopoulos J D, Soljačić M and Zhang B 2018 Superlight inverse Doppler effect *Nature Physics* **14** 1001-5

[11] Boyd D, Stauffer F and Trivelpiece A 1976 Synchrotron radiation from the ATC tokamak plasma *Physical Review Letters* **37** 98

[12] Lu H-W, Hu L-Q, Li Y-D, Zhong G-Q, Lin S-Y and Xu P 2010 Investigation of fast pitch angle scattering of runaway electrons in the EAST tokamak *Chinese Physics B* **19** 125201

[13] Campbell D, Eberhagen A and Kissel S 1984 Analysis of electron cyclotron emission from non-thermal discharges in ASDEX tokamak *Nuclear fusion* **24** 297

[14] Freethy S, McClements K, Chapman S C, Dendy R, Lai W, Pamela S, Shevchenko V F and Vann R 2015 Electron kinetics inferred from observations of microwave bursts during edge localized modes in the mega-amp spherical tokamak *Physical Review Letters* **114** 125004

[15] Santini F, Barbato E, De Marco F, Podda S and Tuccillo A 1984 Anomalous Doppler resonance of relativistic electrons with lower hybrid waves launched in the Frascati tokamak *Physical review letters* **52** 1300

[16] Shustin E, POPOVICH P and Kharchenko I 1971 Transformation of Electron Beam Distribution Function Following Cyclotron Interaction with a Plasma *SOVIET PHYSICS JETP* **32**

[17] Chen Z, Zhu J, Ju H, Du Q, Shi Y, Liang H, Li M and Cai W 2009 Characteristics of the runaway electron beam instability in the HT-7 tokamak *Journal of plasma physics* **75** 661-7

[18] Bin W, Castaldo C, Napoli F, Buratti P, Cardinali A, Selce A, Tudisco O and Team F 2022 First intrashot observation of runaway-electron-driven instabilities at the lower-hybrid frequency range under ITER-relevant plasma-wave dispersion conditions *Physical Review Letters* **129** 045002

[19] Guo Z, McDevitt C J and Tang X-Z 2018 Control of runaway electron energy using externally injected whistler waves *Physics of Plasmas* **25**

[20] ROBERTS C S 1964 Motion of a Charged Particle in a Constant Magnetic Field and a Transverse Electromagnetic Wave Propagating along the Field *PHYSICAL REVIEW*

[21] Lerche I 1968 Quasilinear Theory of Resonant Diffusion in a Magneto-Active Relativistic Plasma *Physics of Fluids* **11** 1720-&

[22] MA R K 1977 Quasi-linear relaxation of runaway electrons in a HF heated tokamak plasma *J. Plasma Physics*

[23] Parail V and Pogutse O 1978 The kinetic theory of runaway electron beam instability in a tokamak *Nuclear Fusion* **18** 303

[24] Zhang R, Liu J, Qin H, Wang Y, He Y and Sun Y 2015 Volume-preserving algorithm for secular relativistic dynamics of charged particles *Physics of Plasmas* **22**

[25] Boris J P 1970 Relativistic plasma simulation-optimization of a hybrid code. In: *Proc. Fourth Conf. Num. Sim. Plasmas,* pp 3-67

[26] Wang Y, Liu J, Qin H, Yu Z and Yao Y 2017 The accurate particle tracer code *Computer Physics Communications* **220** 212-29

[27] Wang Y, Qin H and Liu J 2016 Multi-scale full-orbit analysis on phase-space behavior of runaway electrons in tokamak fields with synchrotron radiation *Physics of Plasmas* **23**

[28] Alikaev V and Parail V 1991 Current drive by electron cyclotron waves *Plasma Physics and Controlled Fusion* **33** 1639-56

[29] Mauel M E 1981 Theory of electron cyclotron heating in the Constance II experiment

[30] Fisch N and Boozer A H 1980 Creating an asymmetric plasma resistivity with waves *Physical Review Letters* **45** 720

[31] Yoshino R, Kondoh T, Neyatani Y, Itami K, Kawano Y and Isei N 1997 Fast plasma shutdown by killer pellet injection in JT-60U with reduced heat flux on the divertor plate and avoiding runaway electron generation *Plasma physics and controlled fusion* **39** 313

[32] Aleynikov P and Breizman B 2015 Stability analysis of runaway-driven waves in a tokamak *Nuclear Fusion* **55** 043014

[33] Spong D A, Heidbrink W, Paz-Soldan C, Du X, Thome K, Van Zeeland M, Collins C, Lvovskiy A, Moyer R and Austin M 2018 First direct observation of runaway-electron-driven whistler waves in tokamaks *Physical Review Letters* **120** 155002

[34] Dendy R O 1987 Classical single-particle dynamics of the anomalous Doppler resonance *Physics of Fluids* **30**

[35] Ginzburg V L 1996 Radiation by uniformly moving sources (Vavilov–Cherenkov effect, transition radiation, and other phenomena) *Physics-Uspekhi* **39** 973

[36] Tamm I E 1959 General characteristics of radiation emitted by systems moving with superlight velocities with some applications to plasma physics *Nobel Lectures* **18** 122-33